THE USE OF NONLINEAR CONSTITUTIVE MODELS FOR CONCRETE IN THE ANALYSIS OF AXISYMMETRIC CONCRETE SHELLS

Mohie Eldin S. Shukry

Structural Engineering Department, Faculty of Engineering,
Alexandria University, Alexandria, Egypt.

ABSTRACT

Three published nonlinear elastic constitutive models for concrete are compared in Initial Stress Finite Element scheme. The models are used in the analysis of axisymmetric concrete shells subjected to combination of radial pressure and axial load; i.e. multiaxial state of compressive stresses. The models used in the present study represent a part of general concrete library (CONLIB) developed by the writer and contains biaxial and multiaxial compression models for concrete. The accuracy and sensitivity of the models vary from those which are satisfactory right through failure to those which are for stresses up to about 80% of the ultimate strength.

INTRODUCTION

Over recent years, several proposed constitutive models for concrete in a multiaxial state of stress have appeared in the literature. Reference 1 provides state of the art report on these models which include nonlinear elastic, elastoplastic, endochronic and hyperelastic models. The nonlinear elastic models have strong empirical basis and enable convenient expression of experimental results of multiaxial tests on solid cylinders in terms of relation between the isotropic invariants of total stresses to total measured surface strains. For practical purposes (e.g. analysis and design), the behaviour of concrete may be considered stress-path independent and nonlinearly isotropic in short term monotonically increasing loading.

The purpose of this paper is to demonstrate the use of three nonlinear elastic models; Kotsovos and Newman [2], Cedolin et al [3] and Ottosen [4], in a finite element scheme involving Initial Stress solutions. It should be noted that these models have been tested separately against experimental results (e.g. see Reference 5).

A concrete shell subjected to an increasing external radial pressure combined with an axial load at its end is used to compare the three models. Axisymmetry in FE methods can be handled as 2-dimensional problem, but stresses and strains occur in three orthogonal directions.

The models developed by Kotsovos and Newman [2] and Cedolin et al [3] have cast in terms of path-independent relation between the isotropic invariants of stress and strain such that:

$$\gamma_o = \frac{\tau_o}{2G_s}, \qquad \epsilon_o = \frac{\sigma_o}{3K_s} \tag{1}$$

where G_s = secant shear modulus

K_s = secant bulk modulus

γ_o = octahedral shear strain; for the axisymmetric case:

$$\gamma_o = \frac{1}{3}\sqrt{(\epsilon_r-\epsilon_z)^2+(\epsilon_z-\epsilon_\theta)^2+(\epsilon_\theta-\epsilon_r)^2+\left(\frac{\gamma_{rz}}{2}\right)^2} \tag{2}$$

τ_o = octahedral shear stress

ϵ_o = octahedral normal (hydrostatic) strain; for the axisymmetric case:

$$\epsilon_o = \frac{\epsilon_r+\epsilon_z+\epsilon_\theta}{3} \tag{3}$$

σ_o = octahedral normal stress

r, Θ and z = radial, circumferential and longitudinal direction respectively.

The model of Ottosen [4] is developed based on secant Young's modulus E_s and secant Poisson's ratio ν_s expressed in terms of nonlinearity index β, which is introduced as a scaler measure of the actual stress state in relation to the failure surface.

BASIC EQUATIONS OF THE MODELS

a) MODEL 1; Kotsovos and Newman [2]

$$G_s = G_o / \left(1 + c \frac{\tau_o}{f_c} \right)^{d-1} \tag{4.a}$$

$$K_s = \sigma_o K^*_s / (\sigma_o + \sigma_i) \tag{4.b}$$

where $K^*_s = K_o / (1 + a(\frac{\sigma_o}{f_c})^{b-1})$; for $\frac{\sigma_o}{f_c} < 2$

$$, K_s^* = K_o / \left(1 + 2^{b-1} b a - 2^b (b-1) a (\frac{\sigma_o}{f_c})^{-1} \right)$$

$$; \quad \text{for } \frac{\sigma_o}{f_c} > 2$$

$$,\sigma_i = \frac{k f_c}{1 + l(\frac{\sigma_o}{f_c})^m} (\frac{\tau_o}{f_c})^n$$

G_o , K_o are initial shear and bulk modulus respectively

G_o , K_o ,a, b, c, d, k, l, m and n are functions of

f_c = uniaxial compressive strength.

This model may be applied up to the ultimate strength only. The post-ultimate strength behaviour of concrete is dependent on testing technique and the most realistic description appears to be a complete and immediate loss of load carrying capacity.

b) MODEL 2; Cedolin et al [3]

$$G_s = G_o(q^{-\gamma_o/r} - s\gamma_o + t) \tag{5.a}$$

$$K_s = K_o(a\, b^{-\epsilon_o/c} + d) \tag{5.b}$$

where $G_o = \frac{E_i}{2(1+\nu_i)}$

$$K_o = \frac{E_i}{3(1-2\nu_i)}$$

E_i and ν_i are initial values of Young's modulus and Poisson's ratio respectively,

a, b, c, d, q, r, s and t are given as constants.

It should be noted that this model is simple in that K_s is considered independent of γ_o and hence τ_o and since only the parameters K_o and G_o need to be derived from the results of uniaxial control tests. Also, in this model, the ultimate strength represents the loss of the load-carrying capacity.

c) MODEL 3; Ottosen [4]

In this model the constitutive relations are dependent on maximum stress surface. The secant values of Young's modulus and Poisson's ratio are given by:

$$E_s = \frac{1}{2}E_i - \beta(\frac{1}{2}E_i - E_f) \pm \sqrt{[\frac{E_i}{2} - \beta(\frac{E_i}{2} - E_f)]^2 + E_i^2\beta[D(1-\beta) - 1]} \tag{6.a}$$

$$\nu_s = 0.36 - (0.36 - \nu_i)\sqrt{1 - (\frac{\beta - 0.8}{0.2})^2} \quad \text{for } \beta > 0.8$$

$$= \nu_i \text{ for } \beta \le 0.8 \tag{6.b}$$

where $\beta = \frac{\text{most compressive principal stress; } \sigma_1}{\sigma_1 \text{ at failure with } \sigma_2, \sigma_3 \text{ are unchanged}}$

(i.e. $\beta = 1$ on the failure surface)

$$E_f = E_c / (1 + 4(A-1)x)$$

$$x = (\frac{\sqrt{J_2}}{f_c})_f - \frac{1}{\sqrt{3}} \quad (x \ge 0$$

E_c secant modulus at uniaxial failure $\frac{c}{\epsilon_c}$

$$A = \frac{i}{E_c}$$

J_2 = second invariant of stress deviator tensor

D = post failure parameter (taken in this study as 0.5)

in this study, A is taken as 2.
Post failure behaviour may be predicted by a suitable choice of the parameter D and by using the negative sign in equation 6-a.

COMPUTATIONAL CONSIDERATIONS

These models are incorporated into structural analysis of plain concrete cylinder subjected to combination of radial external pressure and axial load (i.e. proportional loading). An incremental/iterative procedure is carried out in the analysis. The tangent constitutive matrices in the incremental form of models (1) and (2) can not be obtained simply by replacing the secant moduli in equations 4 and 5 by the tangent moduli. The derived incremental relations [6,7] will exhibit stress-induced anistropy and the tangent matrices may become unsymmetric. This lack of symmetry in the stress-strain matrices is computationally undesirable particularly in finite element analysis.
In this paper, the solution strategy is obtained with the use of Initial Stress algorithm making use of the initial tangent form of the stress-strain relation $[D_0]$; i.e.

$$\{\Delta\sigma\} = [D_o]\ \{\Delta\epsilon\}$$

i.e.

$$\begin{bmatrix}\Delta\sigma_r\\ \Delta\sigma_z\\ \Delta\tau_{rz}\\ \Delta_\theta\end{bmatrix} = \frac{E_i}{(1+\nu_i)(1-2\nu_i)}\begin{bmatrix}(1-\nu_i & \nu_i & 0 & \nu_i\\ \nu_i & (1-\nu_i) & 0 & \nu_i\\ 0 & 0 & \frac{1-2\nu_i}{2} & 0\\ \nu_i & \nu_i & 0 & 0\end{bmatrix}\begin{bmatrix}\Delta_{\epsilon_r}\\ \Delta\epsilon_z\\ \Delta\gamma_{rz}\\ \Delta\epsilon_\theta\end{bmatrix}$$

The solution strategy is briefly as follows:
for the i^{th} iteration of the m^{th} load increment

$$\{a\}_{i,m} = \{a\}_{0,m} + \{\Delta a\}_{i,m} \qquad (8)$$

$$\textit{where}\quad \{a\}_{0,m} = \{a\}_m \quad \textit{with}\quad \{a\}_0 = 0 \qquad (9.a)$$

$$\{\Delta a\}_{i,m} = [K_T]^{-1}\ \{\Delta\psi^*\}_{i-1,m} \qquad (9.b)$$

$$[K_T] = \int_{vol}[B]^T[D][B]\ dV \qquad (9.c)$$

$$\{\Delta\psi^*\}_{i-1,m} = \{\Delta f\}_m + \int_V [B]^T\{\sigma^*\}_{i-1,m}\ dV \qquad (9.d)$$

$$\{\Delta\sigma^*\}_{i-1,m} = \{\Delta\sigma^e\}_{i-1,m} - \{\Delta\sigma^r\}_{i-1,m} \qquad (9.e)$$

$$\textit{elastic stresses}\quad \{\Delta\sigma^e\}_{i-1,m} = [D_0]\{\Delta\epsilon\}_{i-1,m} \qquad (9.f)$$

$$\text{residual stresses}\ \{\Delta\sigma^r\}_{i-1,m} = \{\sigma(\{\epsilon\}_{i-1,m})\} - \{\sigma(\{\epsilon\}_{0,m})\} \qquad (9.g)$$

$$\{\epsilon\}_{i-1,m} = \{\epsilon\}_{0,m} + \{\Delta\epsilon\}_{i-1,m} \qquad (9.h)$$

$$\{\epsilon\}_{0,m} = \{\epsilon\}_m \quad \textit{with}\ \{\epsilon\}_0 = 0 \qquad (9.i)$$

$$\{\Delta\epsilon\}_{i-1,m} = [B]\{\Delta a\}_{i-1,m} \qquad (9.j)$$

This is very similar to the initial stress algorithm commonly used in the conventional solution of elasto-plasticity problems in Finite Element analyses.
The solution of $\{\sigma\}$ given $\{\epsilon\}$ (equation 9.g) could be performed exactly for Cedolin et al model by direct substitution in equations 5.a and 5.b. For Kotsovos model, solution of $\{\sigma\}$ given $\{\epsilon\}$ could be performed to within any sensible order of accuracy specified by the Newton Raphson solution of equation 1 for (σ_o,τ_o) given (ϵ_o,γ_o).
A difficulty is arising in using Ottosen model where explicit determination of $\{\sigma\}$ in terms of $\{\epsilon\}$ is not possible. Therefore, an iterative procedure was carried out using equations 6.a and 6.b in order to obtain the values of the actual stresses corresponding to given values of strains. It should be noted that for this model the determination of the failure surface (i.e. finding the value of β in Eq. 6) was also obtained using Newton-Raphson method. Therefore, the use of this model is relatively more expensive, especially at high stresses, than other models. The procedure used in this study takes the following form:

i) obtain the total stresses $\sigma^1 = \sigma^0 + \Delta\sigma^e$
ii) find the failure surface (the value of β), E_s and ν_s
iii) calculate the actual stresses σ^2
iv) check for convergence
v) if not converged, repeat steps (ii) to (iv).

It is difficult in a finite element analysis, which usually gives strains, to predict the post-failure behaviour using Ottosen model. Ottosen [4] suggested the decrease of E_s by 5% and the increase of ν_s by 0.5% at each step of loading after reaching the failure criterion. However, in

this study, the assumption of no-softening, which corresponds to infinite ductility at failure, was used.

ULTIMATE STRENGTH

Different ultimate strength surfaces were used for the models. The five parameter surface proposed by William and Warnake [8] is used to define the ultimate strength surface for Kotsovos model. The three-dimensional failure criterion based on the four parameter model of Ottosen [9] was used for Ottosen model while the criterion proposed by Cedolin et al [3] was used for their model. For plain concrete shells under external pressure, failure may also be defined by 0.0008 tensile radial strain and not by excessive compressive strain [10] (i.e. limiting strain criterion).

FINITE ELEMENT IDEALIZATION

The finite element idealizations, for some cases studied, are shown in Figure (1). The wall thickness was divided into two eight-node quadrilateral elements with two degrees of freedom per node (radial and longitudinal translations). Three elements across the thickness were used for thicker shells. The half length of the cylinder was divided into nine elements. The ends of the cylinder were considered free restraint. However, the program may incorporate the case of cylindrical wall having different types of end conditions.

CASES STUDIED

The following triaxial compression states were considered in the analysis with different ratios of $\sigma_\theta : \sigma_z : \sigma_r$

(i) hollow cylinders with different wall thicknesses and with σ_z/σ_θ = 0.5 and 1.0.

For a hollow cylinder with infinite length and large values of α ($\alpha = D_o/t > 15$), the stresses in concrete wall are mainly biaxial compression; σ_θ and σ_z and the normal stress in the radial direction σ_r is secondary. The biaxial compression result in a high value of radial tensile strain ϵ_r at the interior face of the cylinder. The principal stresses ratio is about 1 : 0.5 : S (for σ_z/σ_θ = 0.5) or 1 : 1:S (for σ_z/σ_θ = 1.0), where S is small value ranging from zero at the inside surface to about 0.1 at the outside surface.

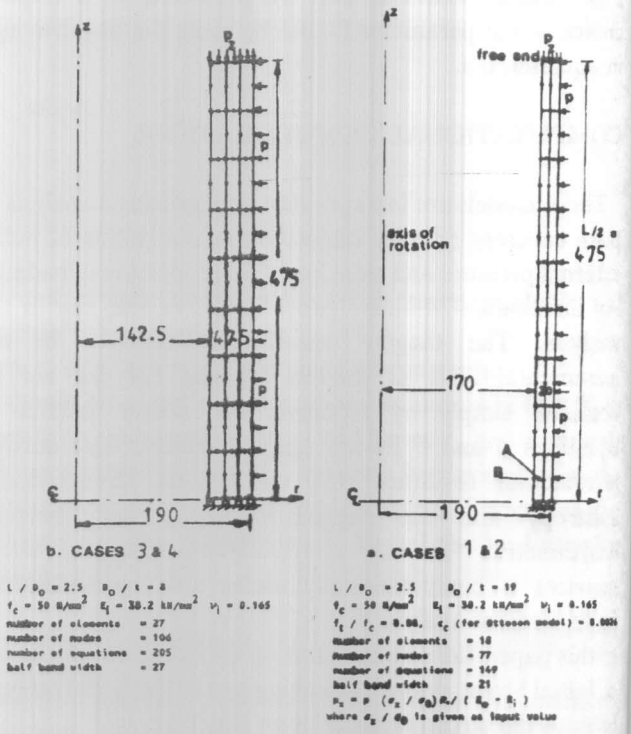

Figure 1. Finite Element layout and concrete properties
a) cases 1 and 2
b) cases 3 and 4.

Also, tensile radial strains occur for shells having smaller values of α but they are limited to the inside surface only. (ii) solid cylinders with σ_z / σ_θ = 0.5 .

Table (1).

CASE	t mm	$\alpha = D_o/t$	σ_z/σ_θ	σ_θ : σ_z : σ_r at mid of inner element	σ_θ : σ_z : σ_r at mid of outer element	σ_θ : σ_z : σ_r at mid-wall
1	20.0	19	0.5	1: 0.5: 0.04	1: 0.5: 0.09	1: 0.5: 0.06
2	20.0	19	1.0	1: 1.0: 0.04	1: 1.0: 0.09	1: 1.0: 0.06
3	47.5	8	0.5	1: 0.4: 0.09	1: 0.6: 0.22	1: 0.5: 0.15
4	47.5	8	1.0	1: 0.9: 0.09	1: 1.1: 0.22	1: 1.0: 0.15
5	95.0	4	0.5	1: 0.5: 0.17	1: 0.6: 0.50	1: 0.5: 0.35
6	95.0	4	1.0	1: 0.8: 0.17	1: 1.2: 0.50	1: 1.0: 0.35
7	solid cylinder		0.5	1 : 0.5 : 1		

Table (1) gives a summary for the cases studied while the concrete properties used in the analyses are given in Figure (1).

Length of all cylinders; L = 950 mm - Outside diameter D_o = 380 mm; giving L/D_o = 2.5

RESULTS OF THE ANALYSIS

Figures (2) to (8) display the main results obtained from the analyses. In the figures, compressive strains and stresses are considered to be positive. These results include the following:

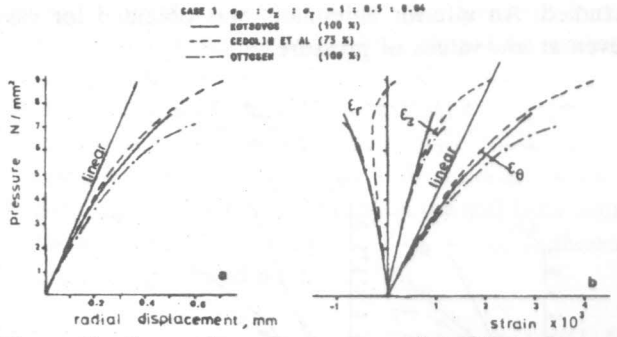

Figure 3. Cases 1: a- pressure-radial displacement relationship b) pressure-strains relationship.

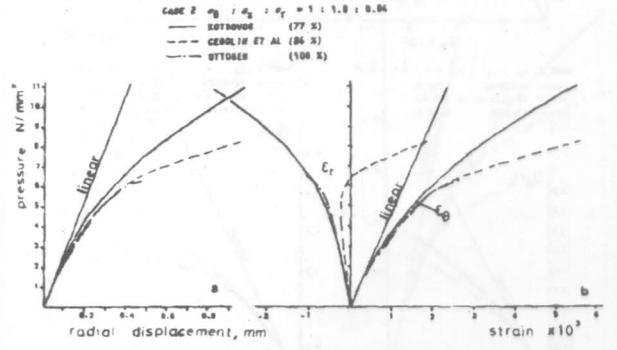

Figure 4. Cases 2: a- pressure-radial displacement relationship b) pressure-strains relationship.

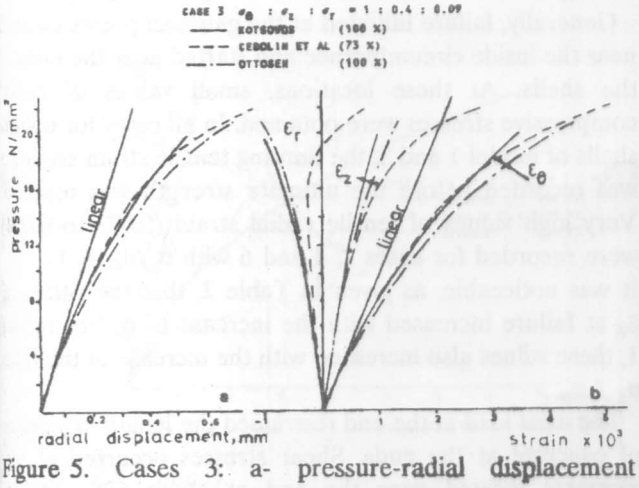

Figure 5. Cases 3: a- pressure-radial displacement relationship b) pressure-strains relationship.

1) circumferential stress-strain relationship for all the cases studied. The values of strains and stresses are given near the inside surface of mid-length of the shell (point A in Figure (1))
2) pressure- strains relationship
3) pressure- inside radial deformation (near mid-length of the shell, point B in Figure (1)) relationship. All the shells were analyzed up to the ultimate strength except that for some cases of model 1 (cases 2, 4 and 6) and all the cases of model 2, high values of tensile radial strains (model 1) and small values of tensile radial stresses (model 2) were obtained without failure of the shells. The percentage given in parentheses in the figures represent the percentage of the ultimate strength at which the analyses were terminated. These values are also given in Table (2), which provides a summary for the main results at the ultimate strength or at the end of the analysis for each case studied.

Table (2)

α	σ_z/σ_θ	KOTSOVOS				CEDOLIN ET AL				OTTOSEN			
		P_i N/mm²	$\varepsilon_\theta \times 10^3$	σ_θ/f_c	% FAIL	P_i N/mm²	$\varepsilon_\theta \times 10^3$	σ_θ/f_c	% FAIL	P_i N/mm²	$\varepsilon_\theta \times 10^3$	σ_θ/f_c	% FAIL
19	0.3	7.0	2.02	1.65	100	9.0	4.18	1.73	73	7.1	3.43	1.46	100
	1.0	11.0	3.43	2.11	77	8.2	3.58	1.31	54	8.4	2.65	1.31	100
8	0.3	21.0	3.90	1.60	100	22.0	5.18	1.62	73	20.3	4.32	1.76	100
	1.0	20.0	7.09	2.41	77	20.0	6.95	1.63	61	20.0	3.91	1.73	100
4	0.3	40.0	4.01	2.00	100	42.0	9.73	1.82	64	79.0	9.74	3.18	100
	1.0	60.0	8.68	2.90	75	60.0	18.12	2.15	69	79.0	8.71	3.12	100
∞	0.3	200.0	16.44	4.90	44	100.0	9.41	1.86	39	250.0	8.09	3.92	46

With regard to the structural response of the shells (characterized by the pressure-radial displacement relationship), there was remarkable agreement between the deformations predicted by both model 1 and model 3 for all the cases, especially case 4 Figure (5), case 5 Figure (6) and case 6 Figure (7). Also, the strains predicted by these two models were nearly consistent for all cases.

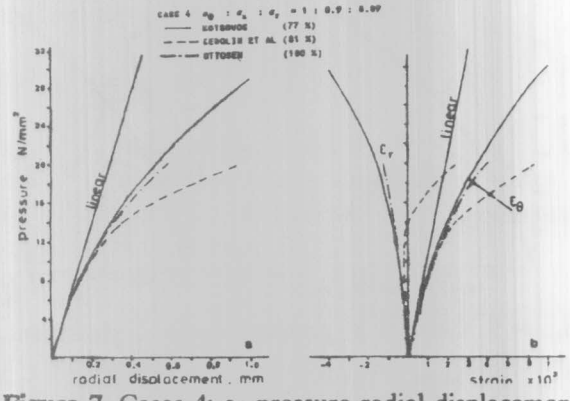

Figure 7. Cases 4: a- pressure-radial displacement relationship b) pressure-strains relationship.

The deformations predicted by model 2 agreed well with those predicted by other models only for cases 1 and 3 (with σ_θ/σ_z = 0.5). For the other cases, this model predicted less stiff behaviour for values of σ_θ / f_c higher than about 1.2 (corresponding to 70% of the ultimate strength for cases 2 and 4 and 58% of the ultimate strength for cases 5 and 6). At these loading levels, the tensile radial strain at the inside surface started to reduce until it finally changed into compressive strain, as shown in the figures, accompanied by a remarkable increase in circumferential and longitudinal strains. In addition, the results of deformation and strains obtained for case 7 (with stress ratio = 1:0.5:1) were unexpected. At a very low pressure (p = 40 N/mm^2), the circumferential strain started to increase rapidly compared with that for other models as shown in Figure (8-g).

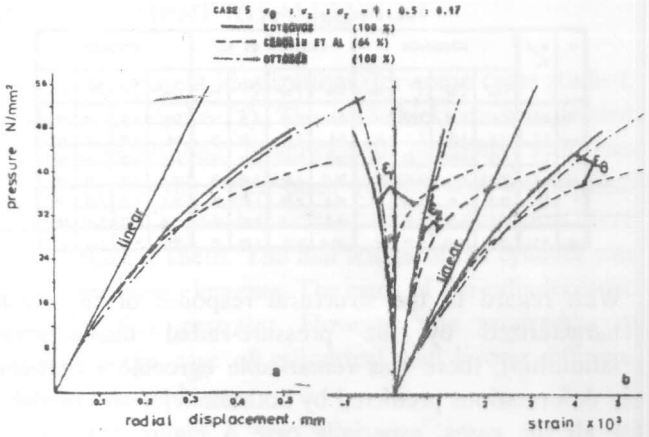

Figure 8. Cases 5: a- pressure-radial displacement relationship b) pressure-strains relationship.

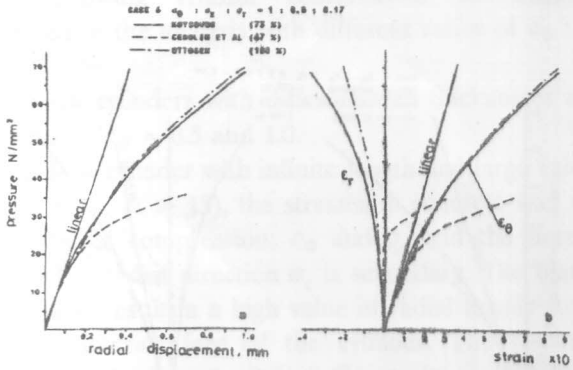

Figure 9. Cases 6: a- pressure-radial displacement relationship b) pressure-strains relationship.

The stress-strain relationship as predicted from models 1 and 3 was consistent (especially for cases 4, 5 and 6) until the failure criterion for model 3 was reached (i.e. β = 1) at the inside surface of the shells (these load levels are indicated in Figure (8) by solid points). Above this loading level, the stress-strain relationship of model 3 became more nonlinear until the overall failure occurred. As shown in Figure (8), model 2 predicted less stiff behaviour compared with other models for most cases studied. An inferior agreement was obtained for case 7 even at low values of pressure.

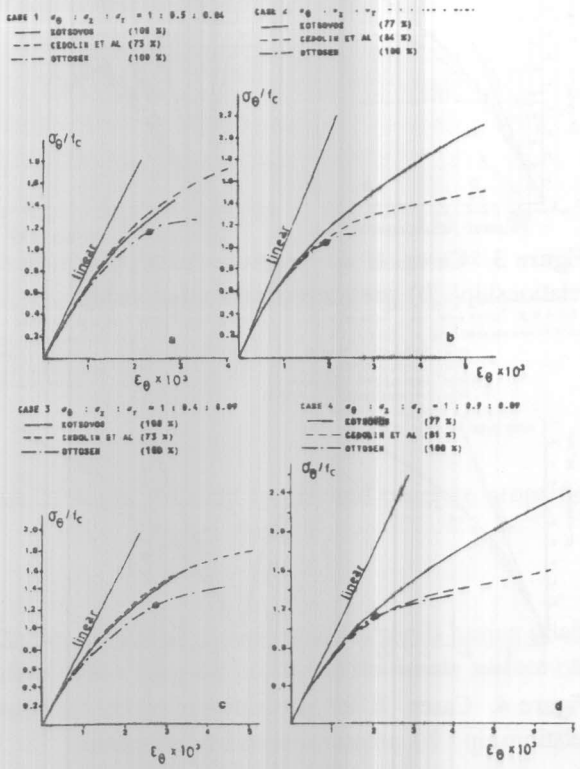

Figure 10. Stress-stain relationship (a to g).

Generally, failure initiated at the gaussian points located near the inside circumference and started near the ends of the shells. At these locations, small values of radial compressive stresses were obtained. In all cases for hollow shells of model 1 and 3, the limiting tensile strain criterion was recorded before the ultimate strength was reached. Very high values of tensile radial strain (0.003 to 0.004) were recorded for cases 2, 4 and 6 with σ_z/σ_θ = 1.0.
It was noticeable, as given in Table 2, that the values of ϵ_θ at failure increased with the increase of α. For model 1, these values also increased with the increase of the ratio σ_z / σ_θ .

The axial load at the end restrained the length expansion of concrete at the ends. Shear stresses occurred at the elements located near the end at about 60% of the ultimate strength. The magnitude of the shearing stresses

decreased with the increase in distance from the ends. By the increase of loading, shear stresses extended to the mid-length of the shells. High values of shear stresses (about 10 N/mm^2) were obtained for cases 6 and 7, while for other cases, the maximum shear stress recorded was about 3.5 N/mm^2 .

The failure criterion developed by William and Warnake (which is used to define failure for Kotsovos model) depends on five parameters which should be evaluated from experimental results. In this study, these parameters were deduced from the tests carried out by Choate [7] on plain concrete hollow cylinders subjected to external pressure only and provided with stiff end diaphragms; i.e. with $\sigma_z / \sigma_\theta = 0.5$. This could explain the stiff behaviour of shells in cases 2, 4 and 6 with $\sigma_z / \sigma_\theta = 1.0$, sa shown in Figures. (8-b, 8-d and 8-f)).

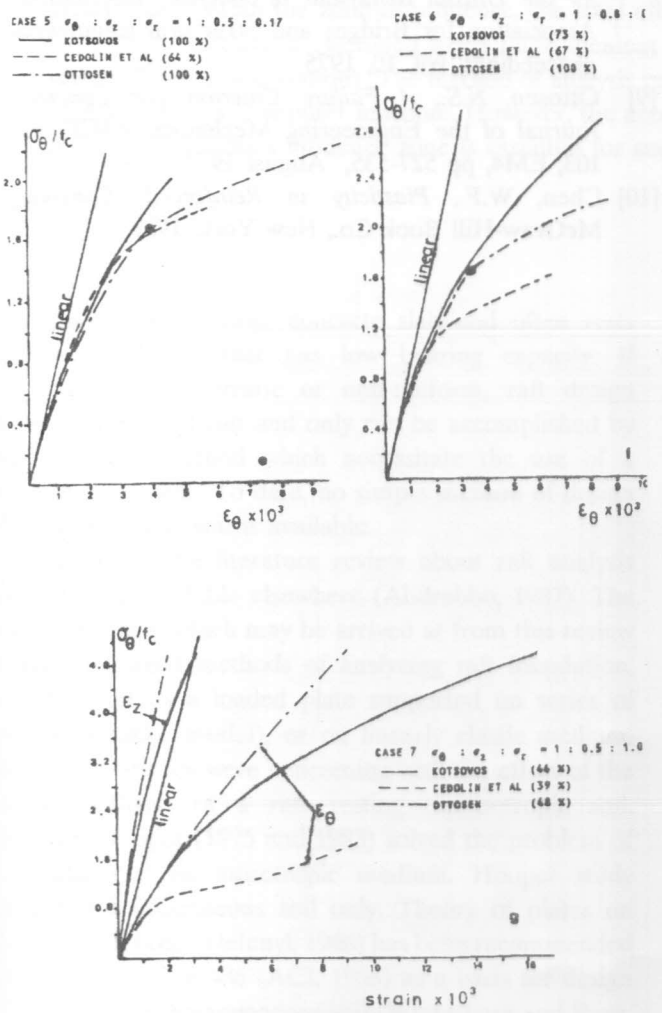

Figure 8. (Canted).

Case 7 (with stress ratio 1 : 0.5 : 1), was analyzed to about 50% of the ultimate strength due to the very high hydrostatic stress component (with σ_{oct} = 4.2 f_c at p = 250 N/mm^2) which increased the ultimate strength of the shell.

The Cedolin et model was developed for conditions not too close to failure [1] since the value of K_s (Eq. 5) is independent of γ_{oct} . This model is based on experimental data on concrete cylinders and cubes with f_c ranging from 7 to 34 N/mm^2 . Case 7 was analyzed to only a pressure of 100 N/mm^2 (compared with p = 250 N/mm^2 for the other two models) and then the analysis was terminated due to large values of radial displacement and circumferential strains.

CONCLUSIONS

It is not the purpose of this paper to check the validity of the models studied herein, but it is to demonstrate their use in the structural analysis of plain concrete shells with different combinations of stress ratios. Based on the results obtained from the analyses, the following general conclusions could be made:

(1) Cedolin et al model [3] is the simplest with regard to its use in FE programming. However, it is limited to about 70 to 80% of the ultimate strength when large deformation and strains occurred without failure of shells. It compared well with other models for hollow shells having σ_z / σ_θ = 0.5. It failed to predict a proper behaviour for solid cylinder with stress ratio = 1: 0.5: 1.

(2) Kotsovos and Newman model [2] worked well for most cases studied. It predicted stiff behaviour for shells having σ_z / σ_θ = 1.0 where no failure was reached.

(3) Ottosen model [4] is very expensive when used in FE programming and also in the post-failure modelling. It predicted well all the cases up to failure.

4- Generally, up to stress level σ_θ / f_c = 0.8 to 1.0, very small differences occurred in deformation and strains for the three models studied.

NOTATION

{a}	nodal displacement vector
{Δa}	incremental nodal displacement vector
[B]	matrix describes strain-displacement relationship
D_o	outside diameter of the shell
[D]	matrix describes stress-strain relationship
{f}	external load vector
$[K_T]$	tangent global stiffness matrix
p	external pressure N/mm^2
p_z	axial load at ends of the shell, N/mm^2

R_i	inside radius
R_o	outside radius
t	wall thickness
γ_{rz}	shear strain in r-z plane
ϵ_r, ϵ_z, ϵ_θ	radial, longitudinal and circumferential strain
σ_r, σ_z, σ_θ	radial, longitudinal and circumferential stress
τ_{rz}	shear stress in r-z plane
$\{\Psi^*\}$	equilibrium error vector

REFERENCES

[1] *Finite Element Analysis of Reinforced Concrete* State of theart report, ASCE, 1983.

[2] Kotsovos, M.D. and Newman, J.B., *Generalized Stress-Strain Relations for Concrete*, Journal of the Engineering Mechanics, ASCE, vol. 104, EM4, pp 845-866, August 1978.

[3] Cedolin, L., Crutzen, Y.R.J. and Dei Poli, S., Triaxial Stress-Strain Relations for Concrete", Journal of the Engineering Mechanics, ASCE, vol. 103, EM3, pp 423-439, June 1977.

[4] Ottosen, N.S., *Constitutive Models for Short-Term Loading of Concrete*", Journal of the Engineering Mechanics, ASCE, vol. 105, EM1, pp 127-141, Feb. 1979.

[5] *Concrete Under Multiaxial States of Stress-Constitutive Equations for Practical Design*, Comite Euro-international du Beton, Bulletin d'information No.156, June 1983.

[6] Murray, D.W., *Octahedral Based Incremental Stress-Strain Matrices*", Journal of the Engineering Mechanics, ASCE, vol. 105, EM4, pp 501-513, August 1979.

[7] Choate, P.R., *Multiaxial Behaviour of Concrete in Shells Subjected to External Pressure*, Ph.D. Thesis, University of Manchester, 1984.

[8] William, K.J. and Warnake, E.P., *Constitutive Model for the Triaxial Behaviour of concrete*, International Association for Bridges and Structural Engineering proceedings, vol. 10, 1975.

[9] Ottosen, N.S., *A Failure Criterion for Concrete*, Journal of the Engineering Mechanics, ASCE, vol. 103, EM4, pp 527-535, August 1977.

[10] Chen, W.F., *Plasticity in Reinforced Concrete*, McGraw-Hill Book Co., New York, 1981.